Med Biol Eng Comput
DOI 10.1007/s11517-011-0734-2

ORIGINAL ARTICLE

Analysis of retinal fundus images for grading of diabetic retinopathy severity

M. H. Ahmad Fadzil · Lila Iznita Izhar · Hermawan Nugroho · Hanung Adi Nugroho

Received: 21 July 2010 / Accepted: 11 January 2011

Abstract Diabetic retinopathy (DR) is a sight threatening complication due to diabetes mellitus that affects the retina. In this article, a computerised DR grading system, which digitally analyses retinal fundus image, is used to measure foveal avascular zone. A v-fold cross-validation method is applied to the FINDeRS database to evaluate the performance of the DR system. It is shown that the system achieved sensitivity of >84%, specificity of >97% and accuracy of >95% for all DR stages. At high values of sensitivity (>95%), specificity (>97%) and accuracy (>98%) obtained for No DR and severe NPDR/PDR stages, the computerised DR grading system is suitable for early detection of DR and for effective treatment of severe cases.

Keywords Diabetic retinopathy grading · Foveal avascular zone · Medical image analysis · Retinal fundus images

1 Introduction

Diabetic retinopathy (DR) is a sight threatening complication due to diabetes mellitus that affects the retina. DR severity can be classified into five levels, namely no DR, mild non-proliferative diabetic retinopathy (NPDR), moderate NPDR, severe NPDR and proliferative diabetic retinopathy (PDR) [8]. According to National Eye Database 2007, among 10,856 Malaysian populations with diabetes, 36.8% has any form of DR, of which 7.1% comprises proliferative diabetic retinopathy [16].

The determination of DR severity is important in treating the disease. At present, an International clinical diabetic retinopathy disease severity scale shown in Table 1 is used in grading of DR [8]. Using the International clinical diabetic retinopathy disease severity scale, an ophthalmologist needs to observe and determine DR-related abnormalities present in the retinal fundus image.

The above pathology-based method is time consuming and often requires fluorescein angiograms for accurate diagnosis. It requires highly trained and skilled clinicians to perform the DR severity grading method.

There are a number of automatic detection systems for DR that are based on one or more features such as blood vessels, exudates, microaneurysms, texture and distances (between the exudates and foveas) reported in scientific literatures [21, 24, 30, 37, 39, 40]. These systems use different classifiers for different type of features. Yun et al. [40] reported the use of area and perimeter features of the RGB components of blood vessels in retinal fundus images with feed-forward neural network classifiers to determine DR stages—normal, mild moderate NPDR, severe NPDR and PDR stages. The system achieved an average efficiency of 84%, sensitivity of 90% and specificity of 100%. Nayak et al. [30] proposed a neural network system based on area of exudates, blood vessels and texture parameters to classify into normal, NPDR and PDR stages. The system achieved a detection accuracy of 93%, sensitivity and specificity of 90 and 100%, respectively. In Kahai et al. [23] a Bayes decision support system with optimality criteria is used to identify early stages of DR based on microaneurysms with a sensitivity of 100% and specificity of 67%.

M. H. Ahmad Fadzil · L. I. Izhar · H. Nugroho · H. A. Nugroho (✉)
Centre for Intelligent Signal and Imaging Research, Department of Electrical and Electronic Engineering, Universiti Teknologi PETRONAS, Bandar Seri Iskandar, 31750 Tronoh, Perak Darul Ridzuan, Malaysia
e-mail: hanungadin@gmail.com

Published online: 27 January 2011

Table 1 International clinical diabetic retinopathy disease severity scale [8]

Proposed disease severity level	Findings observable upon dilated ophthalmoscopy
No apparent retinopathy	No abnormalities
Mild non-proliferative diabetic retinopathy	Microaneurysms only
Moderate non-proliferative diabetic retinopathy	More than just microaneurysms but less than Severe NPDR
Severe non-proliferative diabetic retinopathy	Any of the following:
	1. >20 intraretinal haemorrhages in each of 4 quadrants.
	2. Definite venous beading in 2 + quadrants.
	3. Prominent intraretinal microvascular abnormalities in 1 + quadrant.
	3. No signs of proliferative retinopathy.
Proliferative diabetic retinopathy	One or more of the following:
	1. Neovascularization
	2. Vitreous/pre-retinal haemorrhage

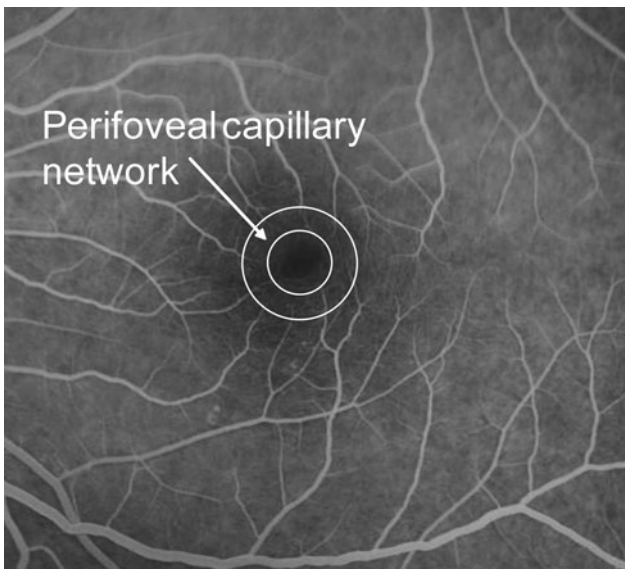

Fig. 1 Fundus fluorescein angiography shows the perifoveal capillary network in FAZ

It has also been reported in medical literature that biologically, the foveal avascular zone (FAZ) enlarges in diabetic retinopathy (DR) cases due to loss of capillaries in the perifoveal capillary network [10, 12, 13]. FAZ is the fovea devoid of capillaries in the macula and can be represented as a dark circle zone without vessels at the centre of macula as shown in Fig. 1 [35]. It varies in size for healthy subjects but usually has a diameter around 500 μm [22, 36, 41] and size of about 0.4 mm^2 [9, 26, 32]. The enlargement of FAZ is not readily observable in retinal fundus images but the effects are seen in fluorescein angiograms for non-proliferative DR (NPDR) and also for proliferative DR (PDR) cases [25].

Early detection of FAZ enlargement at NPDR stage will enable clinicians to advise patients on better metabolic control in order to prevent progression of the disease to PDR stage and visual loss.

In earlier studies, the authors have shown that the enlargement of FAZ is strongly correlated to the progression of DR stages; no DR, mild NPDR, moderate NPDR, severe NPDR to PDR [2, 7, 20]. Digital image enhancement and analysis techniques were developed to enable the effective use of colour fundus images instead of fluorescein angiograms which requires injection of contrasting agents [15].

In this article, an observational clinical study has been conducted to evaluate DR grading system using digital analysis of retinal fundus images only. This avoids the need of injecting contrasting agents as in the case of FFA. A computerised DR monitoring and grading system has been developed for this purpose and will be evaluated for its performance.

2 Methodology

A non-invasive computerised DR system has been developed to implement a DR grading protocol based on FAZ enlargement using retinal fundus images [1–3]. The system composed of an external fundus camera that allows the capture of non mydriatic retinal images (KOWA Non-Myd 7), which is connected to an image processing computer that digitises and analyses retinal fundus images. In this DR grading system, the size of the fundus image is 1936 × 1296 pixels captured at 45°.

3 FAZ analysis for DR grading

The retinal fundus image is digitally analysed to determine the FAZ area for DR grading. The FAZ analysis can be divided into four main processes as shown in Fig. 2.

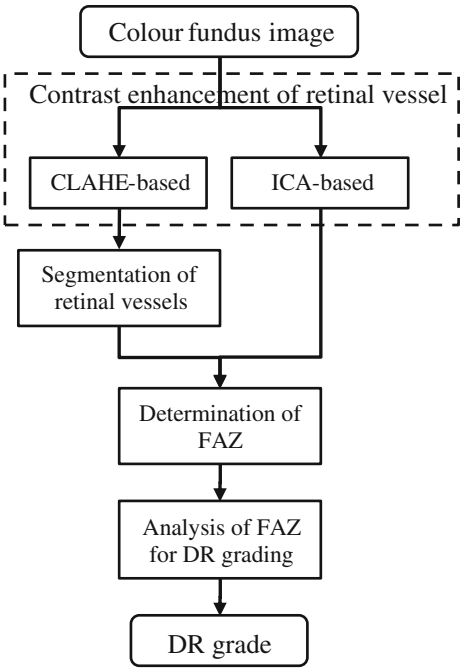

Fig. 2 Flowchart of DR grading algorithm

In the first process, the contrast of the retinal blood vessels against the background image is enhanced. This process is called contrast enhancement of retinal blood vessels. There are two methods of contrast enhancement used in the system, namely Contrast Limited Adaptive Histogram Equalization (CLAHE) [33] and Independent component analysis (ICA) [11, 18].

CLAHE, which is a window (tiles)-based enhancement technique, is applied to increase the contrast of retinal blood vessels to the background in both dark and bright regions as it is more effective in enhancing vessels in varying surroundings evenly and it outperforms other global enhancement methods such as contrast stretching and normal histogram equalisation [33]. The objective of using CLAHE is to apply histogram equalisation within small windows in the image. Grey level values are then distributed evenly within the window to ensure hidden features within the windows more visible. In this study, a window size of 4 × 4 pixels is used. The previous study on method to detect and reconstruct retinal vasculature map is referred [6]. For vessel detection, the fundus image is initially enhanced using a mean filter followed by Contrast Limited Adaptive Histogram Equalization (CLAHE) and followed by bottom-hat morphological transformation to extract retinal vasculature (blood vessels). Background noise removal followed by contrast stretching is then carried out to reduce unwanted line features in the background due to morphological transformation.

ICA is a technique to determine the original signals from mixtures of several independent sources [11, 18]. In this case, enhancement of the low contrast of retinal blood vessels in the digital fundus image is performed by determining the retinal pigments makeup, namely haemoglobin, melanin and macular pigment using independent component analysis. Independent component image owing to haemoglobin obtained exhibits higher contrast retinal blood vessels [4, 5]. Using the CLAHE-enhanced image, the FAZ is determined by selecting centre point at the macula followed by automatic vessel end points locations around the macula. The automatic algorithm is based on nearest distance from the centre point.

The second process is to segment retinal blood vessels in the fundus image. The segmentation process is performed based on Otsu's thresholding [31]. Otsu uses between-class variance as the measure of separability between classes. The method utilises histogram information derived from the input image. In order to evaluate the threshold value for segmentation, the between-class variance is used as a discriminant measure of class separability. The threshold value which optimizes the between-class variance is chosen.

The third process is to detect and select retinal blood vessel end points at perifoveal capillary network to determine and calculate the FAZ area by connecting the end points of retinal blood vessels. The detection of the retinal blood vessel end points is performed by detecting all nearest points to the centre of macula. FAZ area is formed by connecting the detected points that encircle the perimeter of macula. In practice, the following procedure is implemented. A point representing the centre of the macular region is initially chosen and a square area of 600 × 600 pixels centred at this point is cropped. Next, segmented pixels resulted from the second process are grouped into objects (object labelling) using 3 × 3 neighbourhood. Then, the distances between the centre point and all of pixels in the labelled objects are measured. The end point is defined as the pixel with the shortest distance to the centre point for a particular labelled object. Twelve equal radial segments from the centre point are created. Within each radial segment, the end points with the minimum distance from the centre, r_i, are selected. The selected end points are only used if the distance is less than the mean distance of all end points. The selected end points are connected to form the FAZ area. The area of the determined FAZ region is computed below.

$$A(S) = \sum_{i=0}^{i_{\max}} \sum_{j=0}^{j_{\max}} I(x_i y_j) \tag{1}$$

$I(x,y)$ is 1 if the pixel is within the shape, $(x,y) \in S$, and 0 otherwise.

In the last step, a Gaussian Bayes classifier is used to determine DR severity based on the measured FAZ area (in

pixels) obtained from digital retinal fundus images. The classifier uses Bayes theorem for pattern classification and assumes that the classes have Gaussian distribution [14, 29, 34].

In a case of Gaussian Bayes classifier, if class ω_a and ω_b are modelled by Gaussian distribution with mean μ_a and μ_b and variances σ_a^2 and σ_b^2, the log posterior probability ratio (LPPR) can be written as

$$\log \frac{P(\omega_a|x)}{P(\omega_b|x)} = -\frac{1}{2}\left(\frac{(x-\mu_a)^2}{\sigma_a^2} - \frac{(x-\mu_b)^2}{\sigma_b^2} + \log \sigma_a^2 - \log \sigma_b^2\right) + (\log P(\omega_a) - \log P(\omega_b)) \quad (2)$$

If the LPPR is greater than 0, then data x belongs to class ω_a. Otherwise, data x belongs to class to class ω_b [34].

For calibration of DR grading system, the ophthalmologists of Hospital Selayang are blinded to the grading data of the computerised DR system. The grading data from the computerised DR system and ophthalmologists are compared and analysed using MATLAB®, Microsoft Excel® and SPSS® software. The grading ranges of the computerised DR monitoring and grading system are then calibrated for optimum accuracy needed for medical practice.

In grading of DR, the FAZ area (in pixels) is measured for several known DR related fundus images to obtain FAZ area ranges corresponding to the severity of DR. The FAZ area ranges that overlap show progression of the disease from a DR stage to the next. The categories of the ranges used in this study are as follows:

(a) Range 1–No DR stage
(b) Range 2–Progression range from No DR to mild NPDR
(c) Range 3–Mild NPDR
(d) Range 4–Progression range from mild NPDR to moderate NPDR
(e) Range 5–Moderate NPDR
(f) Range 6–Progression range from moderate NPDR to severe NPDR/PDR
(g) Range 7–Severe NPDR/PDR

4 V-Fold cross-validation for performance evaluation

In this study, V-Fold cross-validation (VFCV) is used to evaluate the performance of the classifier [19, 28, 38]. The VFCV is chosen since the number of data is quite small to be separated into training and testing data (number of data for moderate NPDR is only 32). The VFCV algorithm divides randomly data set D into V disjoint subsets T_v, $v = 1, 2, 3 \ldots V$ with approximately equal size and iteratively performs the cross-validation V times. *V-1* of the subsets is used as a learning set and the one remaining subset is used as a test set. An average of the results is used to measure the performance of the developed system. The VFCV is also computationally feasible since V can be chosen (generally between 5 and 10). In this study, V is set to 5 (i.e., each subset consists of 20% of total number of data) since the smallest sample size of the DR severity level is 32 (i.e., moderate NPDR) in order to maintain sufficient training sample size.

5 Results

5.1 Analysis of FAZ

According to the flowchart of DR grading algorithm in Fig. 2, a digital colour retinal fundus image is enhanced prior to obtaining a binary retinal blood vessels map. An example of retinal fundus image is shown in Fig. 3a. A CLAHE-based segmented fundus image shown macular region is depicted in Fig. 3b. An alternative retinal blood vessels enhancement based on ICA is performed to give better visualisation of retinal capillary end points in the perifoveal area as depicted in Fig. 3c [4, 5]. The automated segmentation on CLAHE-based image does not always give accurate vessel end points due to the low contrast of the fundus image and the presence of pathologies near the macula (Fig. 3b). To overcome this, the selected end points are overlaid on the ICA-based images for manual processing to obtain the more accurate estimation of vessel end points (Fig. 3c). The obtained vessel end points are then connected to each other for FAZ determination and analysis (Fig. 3d).

6 Statistics of diabetic patients in the observational clinical study

A total 256 patients were involved in the study. The FAZ area is analysed for 315 fundus images (175 No DR, 52 mild NPDR, 32 moderate NPDR, 18 severe NPDR and 38 PDR) and the statistics of the FAZ areas according to DR severity is shown in Table 2. Severe NPDR and PDR cases are grouped together for the analysis as suggested by the ophthalmologists. This is because severe NPDR and PDR cases are clinically treated in a similar manner and thus it is not crucial to distinguish between the two stages. The collected 315 fundus images are saved into a database called Fundus Image for Non-invasive Diabetic Retinopathy System (FINDeRS). This database is currently waiting for medical approval, and will be publicly available thereafter.

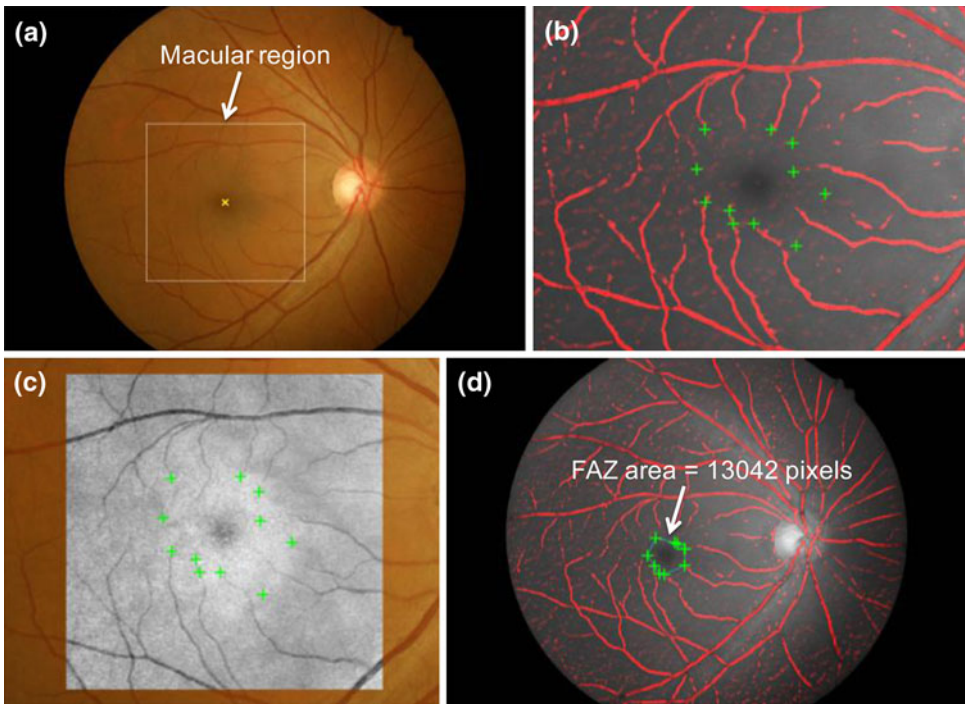

Fig. 3 Fundus image analysis of FAZ. **a** Digital retinal fundus image shown macular region. **b** Extracted retinal vessels with end points in macular region using CLAHE-based method. **c** Vessel end points in macular region are overlaid with the ICA-enhanced image. **d** More accurate estimation of vessel end points shown FAZ area

Table 2 Statistics of FAZ areas for DR grading system

	FAZ area			
	No DR	Mild NPDR	Moderate NPDR	Severe NPDR/PDR
No. of data	175	52	32	56
Mean (pixels)	13644.20	21041.17	27198.31	33933
Std. deviation (pixels)	2727.29	3709.95	3180.89	6787.10
Median (pixels)	13817.00	20177.50	27271.00	3221
Range (pixels)	12543	14200	12226	39507
Minimum (pixels)	6124	14002	21132	27051
Maximum (pixels)	18667	28202	33358	66558

It can be seen from Table 2 that the FAZ mean and median areas increases as the DR stage progresses to a more severe level. Based on the maximum and minimum values of FAZ areas of each DR stage, the ranges of FAZ area for the DR stages overlap. Therefore, an effective and reliable DR severity classification technique has to be developed to handle the overlapping ranges.

7 DR grading using Gaussian Bayes classifier

The LPPR between two selected stages can be computed using the corresponding mean and standard deviation data from Table 2 and applying Eq. 2. From the LPPR, the thresholds of FAZ area ranges for DR grading are determined as shown in Fig. 4. The selected two stages are as follows, No DR and Mild NPDR, Mild NPDR and Moderate NPDR, Moderate NPDR and Severe NPDR/PDR. For example, if LPPR between No DR and Mild NPDR is greater than 0, then the DR grade is categorised as No DR. Otherwise, the DR grade is categorised as Mild NPDR. The LPPR is also calculated for other stages of DR grades.

Table 3 shows the range of FAZ area (in pixels) for the DR grade for different LPPR settings for the Gaussian Bayes classifier.

From Table 3, it can be seen that the ranges of DR grades do not include progression (in between) stages for LPPR = 0. Progression stages are important to give early indication to patients of the DR progression to more severe stages. In Gaussian Bayes classifier, progression stages can be obtained by setting LPPR $\neq$ 0. Table 3 also illustrates the DR grading ranges for three different non-zero LPPR thresholds of the Gaussian Bayes classifier.

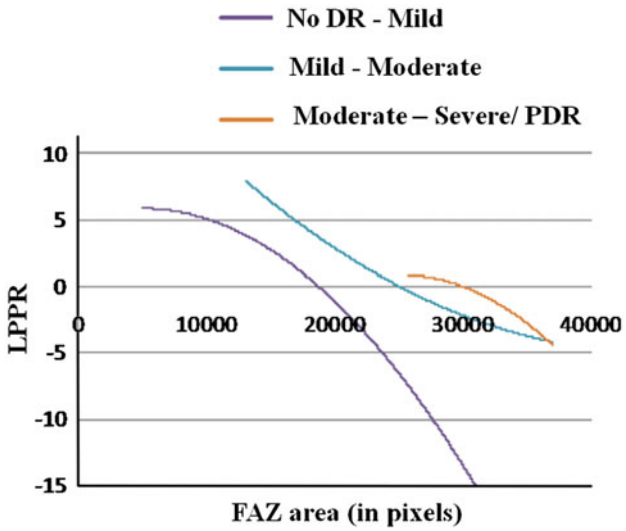

Fig. 4 Log posterior probability ratio (LPPR) for DR grading

The receiver operating characteristic (ROC) analysis is used to find the optimum non-zero LPPR setting. For ROC, the sensitivity and specificity must be determined [17, 27, 42]. Sensitivity measures the proportion of actual positives which are correctly identified and specificity measures the proportion of negatives which are correctly identified. The ROC curve is a plot of sensitivity against 1-specificity across a range of possible thresholds. In addition, accuracy gives overall performance of the classifier.

Using ROC analysis, an optimum threshold is determined for the system by choosing a threshold, which gives an operating point that lies nearest to the reference point. Based on the nearest distance between an operating point and the reference point in the ROC curve, the optimum classifier for each DR stage can be determined. ROC analysis is applied on training data for each iteration of VFCV method to evaluate the performance of the DR system. Using VFCV, data is divided into five subsets to perform five iterations. At each iteration, four subsets are used to train the system while the remaining subset is used test the system. Table 4 shows the performance of the DR system classifier in terms of average sensitivity, specificity and accuracy from the total five iterations.

8 Discussion

As shown in Table 4, the values of sensitivity, specificity and accuracy vary among DR stages. The sensitivity value for the classifier of Mild NPDR has similar value with that of Moderate NPDR (around 84%). This indicates that the classifier has lower ability to correctly detect a patient suffering from Mild or Moderate NPDR when the patient actually having Mild or Moderate NPDR compared with other DR stages (No DR and Severe/PDR stages). It happens since the overlapping FAZ areas in Mild and Moderate NPDR are more than that of other DR stages. It can be minimised by increasing the number of training data for Mild and Moderate NPDR. However, the classifier shows high specificity for Mild and Moderate NPDR (>97%).

Table 3 DR grades with progression stages for different LPPRs

Stage	FAZ area range (pixels)			
	LPPR = 0	−0.25 < LPPR < 0.25	−0.5 < LPPR < 0.5	−0.75 < LPPR < 0.75
No DR	1–18702	1–18405	1–18101	1–17789
Progression no DR to Mild NPDR	–	18406–18731	18102–19278	17790–19558
Mild NPDR	18703–25002	18732–24513	19279–24036	19559–23569
Progression Mild to Moderate NPDR	–	24514–25503	24037–26109	23570–26549
Moderate NPDR	25003–29939	25504–29177	26110–28224	26550–26734
Progression moderate to severe NPDR	–	29178–30593	28225–31175	26735–31703
Severe NPDR/PDR	29940–45431	30594–100000	31176–100000	31704–100000

Table 4 Performance analysis of the DR system classifier

Classifier	Sensitivity (%)	Specificity (%)	Accuracy (%)
No DR–DR	100	97.9 ± 3.1	99.1 ± 1.4
Mild NPDR–other stages	84.1 ± 11.4	99.2 ± 1.0	96.8 ± 1.9
Moderate NPDR–other stages	84.2 ± 16.8	97.1 ± 3.6	95.9 ± 4.5
Severe/PDR–other stages	95 ± 7.5	98.8 ± 1.1	98.1 ± 2.0
System performance (average)	90.81	98.29	97.46

This implies that the classifier is sensitive to other DR stages. The high values of accuracy for all DR stages imply that the system can detect a particular stage with high sensitivity and specificity. The DR system consistently maintains high sensitivity (90.81%), specificity (98.29%) and accuracy (97.46%) for all DR stages. Moreover, high values of sensitivity (>95%), specificity (>97%) and accuracy (>98%) obtained for No DR and Severe NPDR/PDR stages indicate that the DR grading system is suitable for early detection of DR and for effective treatment of severe cases.

For future research, the data can be enlarged to give further confidence of the results. The validity of the proposed DR grading method can be further established by performing cross-validation based on expert opinions. The performance of this DR grading method can also be evaluated for different demographic data.

Acknowledgment The authors would like to acknowledge the contributions of Dr. Nor Fariza Ngah, Dr. Tara Mary George, Dr. Mariam Ismail, Dr. Elias Hussein and Dr. Goh Pik Pin from Department of Ophthalmology, Hospital Selayang for their suggestions and contributions in providing the retinal fundus image data. The research study was funded by the Ministry of Science, Technology and Innovation under the Techno Fund grant TF0206C129. The Clinical Observational Study NMRR–08–942–1997 was approved by the Clinical Research Centre, Ministry of Health, Malaysia.

Conflict of interest None.

References

1. Ahmad Fadzil MH, Izhar LI (2008) A non-Invasive method for analysing the retina for ocular manifested diseases. Patent filing no. PI20083503 September, 2008 ed. Malaysia, v. patent filing no. PI20083503 September, 2008
2. Ahmad Fadzil MH, Lila Iznita I (2009) A non-Invasive method for analysing the retina for ocular manifested diseases. Patent filing no. PCT/MY2009/000025 2009 ed. Malaysia, v. patent filing no. PCT/MY2009/000025 2009
3. Ahmad Fadzil MH, Lila Iznita I (2009) An apparatus for monitoring and grading diabetic retinopathy. Patent filing no. PI20091936 May, 2009 ed. Malaysia, v. patent filing no. PI20091936 May, 2009
4. Ahmad Fadzil MH, Nugroho HA, Venkatachalam PA, et al (2008) Determination of retinal pigments from fundus images using independent component analysis. In: Proceeding of biomed 2008 4th Kuala Lumpur international conference on biomedical engineering vol 21. Springer, Berlin Heidelberg, 2008
5. Ahmad Fadzil MH, Nugroho HA (2009) Retinal vasculature enhancement using independent component analysis. J Biomed Sci Eng 2:543–549
6. Ahmad Fadzil MH, Izhar LI, Venkatachalam PA, Karunakar TVN (2007) Extraction and reconstruction of retinal vasculature. J Med Eng Tech 31:435–442
7. Ahmad Fadzil MH, Lila Iznita I, Nugroho HA (2009) Analysis of foveal avascular zone in color fundus image for grading of diabetic retinopathy. Int J Recent Trends Eng 2:101–104
8. American academy of ophthalmology retina panel. Preferred practice pattern guidelines. Diabetic retinopathy. American Academy of Ophthalmology San Francisco, CA. http://www.aao.org/ppp
9. Bradley A, Applegate RA, Zeffren BS, Heuven WAJ (1992) Psychophysical measurement of the size and shape of the human foveal avascular zone. Ophthal Physiol Opt 12:18–23
10. Bresnick GH, Condit R, Syrjala S et al (1984) Abnormalities of the foveal avascular zone in diabetic retinopathy. Arch Ophthalmol 102:1286–1293
11. Comon P (1994) Independent component analysis, a new concept? Signal Process 36:287
12. Conrath J, Giorgi R, Raccah D, Ridings B (2004) Foveal avascular zone in diabetic retinopathy: quantitative vs qualitative assessment. Eye 19:322–326
13. Conrath J, Valat O, Giorgi R et al (2006) Semi-automated detection of the foveal avascular zone in fluorescein angiograms in diabetes mellitus. Clin Exp Ophthalmol 34:119–123
14. Duda RO, Hart PE, Stork DG (2001) Pattern classification. Wiley, New York
15. Fadzil MHA, Lila Iznita I, Hanung Adi N (2010) Determination of foveal avascular zone in diabetic retinopathy digital fundus images. Comput Biol Med 40:657–664
16. Goh PP (2008) Status of diabetic retinopathy among diabetics registered to the diabetic eye registry, National eye database, 2007. Med J Malaysia 63:24–28
17. Hanley JA, McNeil BJ (1982) The meaning and use of the area under a receiver operating characteristic (ROC) curve. Radiology 143:29–36
18. Hyvarinen A, Oja E (2000) Independent component analysis: algorithms and applications. Neural Networks 13:411
19. Izenman AJ (2008) Modern multivariate statistical techniques: regression, classification, and manifold learning. Springer New York, Berlin
20. Iznita L (2006) Analysis of retinal vasculature and foveal avascular zone for grading of diabetic retinopathy. M.Sc. Thesis, Universiti Teknologi PETRONAS, Electrical and electronics engineering programme. Bandar Seri Iskandar, Malaysia
21. Jelinek HF, Cree MJ, Leandro JJG et al (2007) Automated segmentation of retinal blood vessels and identification of proliferative diabetic retinopathy. J Opt Soc Am A 24:1448–1456
22. John D, Braganza A, Kuriakose T (2006) A study of the foveal avascular zone using the Heidelberg retina angiogram-2 in normal eyes. In: Proceedings 34th all India optometry conference (AIOC 2008) Amritsar, India
23. Kahai P, Namuduri KR, Thompson H (2004) Decision support for automated screening of diabetic retinopathy. Conference on signals, systems and computers, vol 2. Conference record of the thirty-eighth asilomar
24. Kahai P, Namuduri KR, Thompson H (2006) A decision support framework for automated screening of diabetic retinopathy. Int J Biomed Imaging 2006:1–7
25. Khurana AK (2003) Ophthalmology. New Age International Publishers, New Delhi
26. Mansour AM (1990) Measuring fundus landmark. Invest Ophthalmol Vis Sci 31:41–42
27. Metz C (2008) ROC analysis in medical imaging: a tutorial review of the literature. Radiol Phys Technol 1:2–12
28. Micheli-Tzanakou E (2000) Supervised and unsupervised pattern recognition: feature extraction and computational intelligence. CRC Press, Boca Raton
29. Mitchell TM (1997) Machine Learning. McGraw-Hill, New York
30. Nayak J, Bhat P, Acharya UR et al (2008) Automated identification of diabetic retinopathy stages using digital fundus images. J Med Syst 32:107–115

31. Otsu N (1979) A threshold selection method from gray-level histograms. IEEE Transactions on Systems, Man and Cybernetics 9:62–66
32. Parodi MB, Visintin F, Rupe PD, Ravalico G (1995) Foveal avascular zone in macular branch retinal vein occlusion. Int Ophthalmol 19:25–28
33. Pratt WK (1978) Digital image processing. Wiley, New York
34. Rasmussen CE, Williams CKI (2006) Gaussian processes for machine learning. MIT, Cambridge, Mass
35. Richard G, Soubrane Gl, Yannuzzi LA, Courland S (1998) Fluorescein and ICG angiography. Thieme Medical, New York
36. Saini VK, Varma P, Bhaisare V, et al. Foveal Avascular Zone Calculation and its Variation with Different Posterior Segment Diseases and Analysis of its Impact on Best Corrected Visual Acuity. In: Bhattacharyya DD, AIOC 2006. Bhopal, India, 2006; v. 4
37. Sopharak A, Uyyanonvara B, Barman S, Williamson TH (2008) Automatic detection of diabetic retinopathy exudates from non-dilated retinal images using mathematical morphology methods. Comput Med Imaging Graph 32:720–727
38. Stone M (1974) Cross-validatory choice and assessment of statistical predictions. J Royal Stat Soc B 36:111–147
39. Walter T, Klein J-C, Massin P, Erginay A (2002) A contribution of image processing to the diagnosis of diabetic retinopathy-detection of exudates in color fundus images of the human retina. IEEE Trans Med Imaging 21:1236–1243
40. Yun WL, Rajendra Acharya U, Venkatesh YV et al (2008) Identification of different stages of diabetic retinopathy using retinal optical images. Inf Sci 178:106–121
41. Zeffren B, Applegate R, Bradley A, van Heuven W (1990) Retinal fixation point location in the foveal avascular zone. Invest Ophthalmol Vis Sci 31:2099–2105
42. Zweig MH, Campbell G (1993) Receiver-operating characteristic (ROC) plots: a fundamental evaluation tool in clinical medicine. Clin Chem 39:561–577